Heliyon 10 (2024) e36176

Contents lists available at ScienceDirect

Heliyon

journal homepage: www.cell.com/heliyon

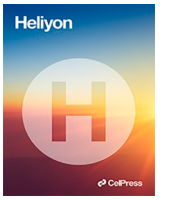

Research article

Puerarin ameliorates high glucose-induced MIN6 cell injury by activating PINK1/Parkin-mediated mitochondrial autophagy

Hongyang Zhu [a,1], You Yu [b,1], Yuting Li [a], Shiyao Chang [a], Yuhui Liu [a,*]

[a] College of Pharmacy, Jiangxi University of Chinese Medicine, Nanchang, China
[b] The First Affiliated Hospital Of Nanchang University, Nanchang, China

ARTICLE INFO

Keywords:
Type 2 diabetes
β-cell dysfunction
Puerarin
Mitochondrial autophagy
Mitochondrial apoptosis

ABSTRACT

The dysfunction of pancreatic β-cells plays a pivotal role in the pathogenesis of type 2 diabetes mellitus (T2DM). Despite numerous studies demonstrating the anti-inflammatory and antioxidant properties of puerarin, the protective effects of puerarin on β-cells remain poorly understood. Hence, this study aimed to explore the effects of puerarin on β-cell dysfunction in a hyperglycemic environment via the PINK/Parkin-mediated mitochondrial autophagy pathway. The alterations in cell viability of MIN6 cells exposed to glucose concentrations of 5 mM, 10 mM, 20 mM, and 30 mM for 24 h, 48 h, and 72 h, respectively, were assessed using the CCK-8 assay to optimize the modeling conditions. Subsequently, cellular insulin secretion was measured using enzyme-linked immunosorbent assay (ELISA), apoptosis rate by flow cytometry, mitochondrial membrane potential alteration by JC-1, cellular ROS production by the DCFH-DA fluorescent probe, and fusion of cellular autophagosomes and lysosomes through adenoviral infection analysis. Furthermore, gene and protein expression levels of the PINK/Parkin-mediated mitochondrial autophagy pathway and mitochondrial apoptosis pathway were assessed using real-time quantitative polymerase chain reaction (RT-qPCR) and Western blot, respectively. Results indicated a significant decrease in MIN6 cell viability following 48 h of exposure to 30 mM glucose concentration. Puerarin intervention markedly attenuated ROS production, restored mitochondrial membrane potential, induced PINK/Parkin-mediated mitochondrial autophagy, suppressed activation of the mitochondrial apoptotic pathway, mitigated apoptosis, and enhanced insulin secretion in a high glucose (HG) environment. The findings of this investigation contribute to a deeper understanding of the precise mechanism underlying the protective effects of puerarin on β-cells and offer a theoretical foundation for advancing puerarin-based therapeutics aimed at ameliorating T2DM.

1. Introduction

Type 2 diabetes mellitus (T2DM) represents a chronic condition marked by aberrant glucose metabolism and distinguished by dysfunction of pancreatic beta cells and insulin resistance [1]. The International Diabetes Federation (IDF) projects a global rise in diabetes prevalence to 537 million by 2030, affecting individuals aged 20 to 79, with an estimated prevalence of 11.3 % [2]. With the escalating numbers and prevalence of diabetes, healthcare systems worldwide will confront an increasingly substantial burden. Studies

* Corresponding author.
E-mail address: 20070962@jxutcm.edu.cn (Y. Liu).
[1] These authors contributed equally to this article.

https://doi.org/10.1016/j.heliyon.2024.e36176
Received 22 April 2024; Received in revised form 10 August 2024; Accepted 12 August 2024
Available online 12 August 2024

have shown that islet dysfunction significantly contributes to hyperglycemia development in T2DM patients, and insulin resistance becomes relevant only when islet dysfunction is present due to compensatory failure [3]. Hence, dysfunction of pancreatic β-cells assumes a pivotal role in the pathogenesis of T2DM. β-cell injury is a critical factor contributing to pancreatic islet β-cell dysfunction. β-cell apoptosis, a specific manifestation of β-cell injury, indicates the extent of β-cell dysfunction. Research has validated that inhibiting β-cell apoptosis enhances insulin secretion and mitigates glucotoxicity in T2DM mice [4].

Studies have demonstrated that elevated glucose levels can induce the accumulation of reactive oxygen species (ROS) in pancreatic islets through various pathways such as glyceraldehyde autoxidation, protein kinase C activation, methylglyoxal formation, glycosylated sorbitol metabolism, hexosamine metabolism, glucuronidation, and oxidative phosphorylation, ultimately leading to β-cell injury [5]. Mitochondria are the primary organelles for ROS generation and are vulnerable to oxidative stress, resulting in mitochondrial damage [6]. Furthermore, damaged mitochondria exacerbate ROS production, elevate mitochondrial membrane permeability, reduce mitochondrial membrane potential, and induce mitochondrial dysfunction [7]. Research has indicated that mitochondrial dysfunction is intricately linked to apoptosis, with damaged mitochondria inducing apoptosis via the mitochondrial apoptotic pathway [8]. Mitochondrial autophagy, a cellular mechanism for preserving homeostasis, selectively eliminates damaged or malfunctioning mitochondria, thereby maintaining mitochondrial quality and quantity stabilization and reducing apoptosis [9]. PTEN-induced putative kinase 1 (PINK1) and E3 ubiquitin ligase PARK2 (Parkin) constitute classical pathways governing mitochondrial autophagy regulation. The inner mitochondrial membrane potential diminishes upon mitochondrial damage, accumulating PINK1 on the outer mitochondrial membrane, activating Parkin by phosphorylating its ubiquitin-like domains [7]. Consequently, activated Parkin promotes the ubiquitination of mitochondrial outer membrane proteins, facilitating the interaction between sequestosome 1 (p62) and microtubule-associated protein 1 light chain 3 II (LC3 II), thereby facilitating the progression of mitochondrial autophagy [10]. Yelong Ji et al. demonstrated that enhancing mitochondrial autophagy via the PINK1/Parkin pathway mitigates high glucose (HG)-induced H9C2 cell injury, suppresses cardiomyocyte apoptosis, and alleviates myocardial ischemia/reperfusion (MIR) injury in T2DM [11]. Nonetheless, a dearth of studies confirms the association between HG-induced pancreatic β-cell injury and mitochondrial autophagy regulated by the PINK1/Parkin pathway.

Puerarin, the principal active constituent of the Chinese herb Pueraria montana var. lobata (Willd.) Maesen & S.M. Almeida ex Sanjappa & Predeep is a naturally occurring isoflavonoid [12]. Contemporary research indicates that puerarin possesses anti-inflammatory, antioxidant, insulin-sensitizing, and hypoglycemic properties, rendering it suitable for preventing cardiovascular disease, osteoporosis, inflammatory conditions, liver injury, and diabetes mellitus [13]. Zhipeng Li et al.'s research elucidated that puerarin safeguards β-cells against cobalt chloride (CoCl2)-induced apoptosis and ameliorates compromised glucose-stimulated insulin secretion through the modulation of the phosphoinositide 3-kinase/protein kinase B (Akt) signalling pathway [14]. This indicates that puerarin exerts a protective effect on β-cells in hypoxic conditions. Nonetheless, there is a lack of research regarding the effects of puerarin on β-cells in HG environments.

This study aimed to establish an *in vitro* model of pancreatic β-cell injury using HG concentration and investigate puerarin's effect on HG-induced β-cell injury. Furthermore, we investigated the interplay between PINK1/Parkin-mediated mitochondrial autophagy and apoptosis and the potential mechanism underlying puerarin's protective effect against HG-induced β-cell injury.

2. Materials and methods

2.1. Materials

Puerarin (MKCN0894) was purchased from Sigma-Aldrich Corporation (St. Louis, MO, USA). D-glucose anhydrous (318Z023), DMEM oligosaccharide medium (2310001), and JC-1 mitochondrial membrane potential assay kit (2310004) were purchased from Solarbio Science & Technology Co., Ltd. (Beijing, China), Bax Rabbit mAb (14796, 1:1000), Cytochrome *c* Rabbit mAb (11940, 1:1000), SQSTM1/p62 (23214, 1:1000), and β-actin antibody (4967, 1:1000) were purchased from Cell Signaling Technology (Danvers, MA, USA). Anti-Bcl-2 antibody (ab196495, 1:1000), Anti-Caspase-3 antibody (ab79123, 1:1000), Anti-Caspase-9 antibody (ab184786, 1:1000), Anti-LC3B antibody (ab192890, 1:2000), and Anti-Beclin-1 antibody (ab207612, 1:1000) were purchased from Abcam (Cambridge, MA, USA). PINK1 Antibody (85h3726, 1:1000), Parkin Antibody (13v0541, 1:1000), Phospho-PINK1 (Ser228) Antibody (77h3625, 1:1000), and Phospho-Parkin (Ser65) Antibody (17h5111, 1:1000) were purchased from Affinity Biosciences (Cincinnati, OH, USA). The mCherry-EGFP-LC3 adenovirus (AP23110202) was purchased from Hanheng Biotechnology Co. (Shanghai, China). The ROS detection kit (S0033S) was purchased from Beyotime Biotechnology (Shanghai, China).

2.2. Cell culture

Mouse islet β-cells (MIN6 cells) were procured from the BeNa Culture Collection. Rigorous screening via RT-qPCR on July 5, 2023 confirmed the absence of mycoplasma contamination. Normal-growing cells were cultured in DMEM low-glycemic medium supplemented with 10 % fetal bovine serum (Gibco, Australia), 100 U/ml penicillin, 100 μg/L streptomycin, and 5 mM glucose and maintained in an incubator at 37 °C with 5 % carbon dioxide. The HG-induced MIN6 cell injury model was established by culturing the cells in a medium containing 30 mM glucose while maintaining the remaining culture conditions identical to normal-growing cells. The subsequent experiments used cells from the 3rd to the 6th subcultures during their logarithmic growth phase.

2.3. Drugs and treatment

Puerarin was dissolved in DMSO to achieve a concentration of 200 mM and aliquoted for storage at −80 °C. For the treatment, the stock solution of puerarin was diluted with a complete medium at the corresponding glucose concentration as required by the experimental conditions (the dilution was more significant than 1000-fold), ensuring that both the puerarin and medium acted on MIN6 cells simultaneously.

2.4. Cell viability

MIN6 cells were seeded in 96-well plates at a density of 5000 cells per well and cultured for 24 h. After 24 h of normal growth, MIN6 cells were treated with a medium containing 5 mM, 10 mM, 20 mM, and 30 mM glucose for 24, 48, and 72 h, respectively. The old culture medium was discarded and replaced with fresh medium. Subsequently, 10 μl of Cell Counting Kit-8 (CCK-8) reagent was added to each well, and the cells were incubated in a 37 °C incubator, protected from light, for 3–4 h. Absorbance was then measured at 450 nm using an ELX-800 enzyme marker (BIOTEK, Winooski, VT). The effect of puerarin on the viability of normal-growing MIN6 cells was assessed by treating the cells with varying concentrations of puerarin (0, 10, 20, 40, 60, 80, 100, and 200 μM) for 48 h, followed by the same procedure. Furthermore, an identical protocol was employed to assess the impact of hypertonicity and DMSO on the viability of MIN6 cells. MIN6 cells were seeded into 96-well plates at a density of 5000 cells per well. Once the cells had fully adhered to the plate, they were categorized into four groups: normal-growing MIN6 cells (control), MIN6 cells in a hypertonic environment, HG-induced MIN6 cells, and HG-induced DMSO-treated MIN6 cells. Following the aforementioned experimental procedure, absorbance measurements for cell viability were taken after 48 h.

2.5. Enzyme-linked immunosorbent assay

MIN6 cells were seeded in 6-well plates at a density of 3 × 10ˆ5 cells per well. After complete cell attachment, the cells were divided into normal-growing cells (control) and HG-induced MIN6 cells. The culture supernatant was collected after treatment with puerarin (10 μM, 20 μM, and 40 μM) for 48 h. Subsequently, centrifugation was carried out at 2000 rpm for 20 min at 4 °C to remove floating cells from the culture supernatant, and the supernatant was carefully collected. The procedures outlined in the insulin test kit manual (Nanjing Jiancheng Technology, Jiangsu, China) were strictly adhered to, and absorbance at 450 nm was measured using enzyme labeling instruments.

2.6. Flow cytometry analysis

MIN6 cells were seeded in 6-well plates at a density of 3 × 10ˆ5 cells per well. Once the cells had fully adhered, they were divided into normal-growing cells (control) and HG-induced MIN6 cells. Following 48 h of puerarin intervention, the cells were trypsinized to detach them from the Petri dish, washed via centrifugation in pre-cooled PBS, and collected, including those in the culture supernatant, as per the instructions of the Apoptosis Detection Kit (MultiSciences (Lianke) Biotech, Shanghai, China). Cells were then resuspended in 500 μl of 1 × Binding Buffer working solution. 5 μl of Annexin V-FITC and 10 μl of PI were added to each tube, followed by gentle vortexing and mixing. The mixture was subsequently shielded from light and incubated at room temperature for 5 min for flow cytometric analysis.

2.7. JC-1 staining

MIN6 cells were seeded in 24-well plates at a density of 4 × 10ˆ4 cells per well. After the cells had fully adhered, they were divided into normal-growing cells (control) and HG-induced MIN6 cells. Following 48 h of puerarin treatment, the procedure outlined in the JC-1 Mitochondrial Membrane Potential Assay Kit (Beijing, China) was followed. Initially, the culture medium was discarded, followed by the addition of the pre-configured JC-1 staining working solution. Cells were then incubated in a cell culture incubator at 37 °C for 30 min. Subsequently, cells were washed twice with 1 × JC-1 staining buffer, and a fresh culture medium was added for visualization under a fluorescence microscope. The acquired images were analyzed using ImageJ software. For each group, nine fluorescence images were imported. The red and green fluorescence channels were separated, appropriate thresholds were set, and the average fluorescence intensities of the red and green channels were analyzed. Subsequently, the ratio of these intensities was calculated.

2.8. ROS activity detection

MIN6 cells were seeded in 24-well plates at a density of 4 × 10ˆ4 cells per well. After the cells had fully adhered, they were divided into normal-growing cells (control) and HG-induced MIN6 cells. Following 48 h of puerarin treatment, the culture medium was removed. Subsequently, the DCFH-DA fluorescent probe was diluted to a concentration of 10 μM in serum-free culture medium at a ratio of 1:1000 and incubated for 20 min at 37 °C in a cell culture incubator. The cells were rinsed three times with serum-free cell culture medium, replenished with fresh culture medium lacking phenol red, and examined under a fluorescence microscope. The acquired images were analyzed using ImageJ software. For each group, nine fluorescence images were imported. The green fluorescence channel was separated, and the total fluorescence intensity was analyzed by setting the appropriate threshold.

Table 1
Primer sequences.

Gene	Primer (5′–3′)
β-actin	F 5′-CATTGCTGACAGGATGCAGA-3′
	R 5′-CTGCTGGAAGGTGGACAGTGA-3′
Ins	F 5′-TGAAGTGGAGGACCCACAAGTG-3′
	R 5′-TACAATGCCACGCTTCTGCTG-3′
Bax	F 5′-GCAGCGGCAGTGATGGAC-3′
	R 5′-GCAAAGTAGAAGAGGGCAACC-3′
Bcl-2	F 5′-ACCCTCCTGATTTTTCCTCCACCTA-3′
	R 5′-AATACATAAGGCAACCACACCATCG-3′
Cyt-c	F 5′-ATAGAACCAAGAAGGAGATTGACCA-3′
	R 5′-TACAGACACCTATCAGAATAACCCA-3′
Caspase-3	F 5′-GACTTCTCTGACTATCGTCGTGCTG-3′
	R 5′-CGCATAAGCAACACCCACAGTAGTA-3′
Caspase 9	F 5′-GGCTGTCTACGGCACAGATGGA-3′
	R 5′-CTGGCTCGGGGTTACTGCCAG-3′
PINK1	F 5′-GCTTGCCAATCCCTTCTATG-3′
	R 5′-CTCTCGCTGGAGCAGTGAC-3′
Parkin	F 5′-ACCATCAAGAAGACCACCAAG-3′
	R 5′-GTTCCACTCACAGCCACAG-3′
Beclin-1	F 5′-GAGCCATTTATTGAAACTCGCCA-3′
	R 5′-CCTCCCCGATCAGAGTGAA-3′
LC3II	F 5′-CGCTTGCAGCTCAATGCTAAC-3′
	R 5′-TCTCTCACTCTCGTACACTTCG-3′
p62	F 5′-ATCCGCTACCTCATCCCCCAAC-3′
	R 5′-GCAGACCATCCGTCACCAGATTG-3′

2.9. Mito-Tracker Green and Lyso-Tracker Red co-localization analysis

MIN6 cells were seeded in 24-well plates at a density of 4 × 10^4 cells per well. After the cells had fully adhered, they were divided into normal-growing cells (control) and HG-induced MIN6 cells. Following 48 h of puerarin treatment, subsequent experiments were conducted. Working solutions of Mito-Tracker Green and Lyso-Tracker Red were prepared according to the manufacturer's instructions. They were diluted with a complete medium under light-avoidance conditions to achieve final concentrations of 50 nM and 100 nM, respectively. The solutions were warmed in a 37 °C water bath and allowed to equilibrate. After removing the culture medium, the cells were washed with PBS and treated with the Mito-Tracker Green working solution. Subsequently, the cells were incubated at 37 °C for 30 min. After the incubation, the Mito-Tracker Green working solution was carefully aspirated, the cells were washed once with PBS, and then the Lyso-Tracker Red working solution was added. Incubate at 37 °C for 60 min. The culture medium was refreshed, and the cells were observed under a fluorescence microscope. The acquired images were analyzed using ImageJ software. For each group, nine fluorescence images were imported. The red and green fluorescence channels were separated, and their correlation was analyzed through co-localization and quantified using Pearson's coefficients.

2.10. mCherry-EGFP-LC3 adenovirus infection

MIN6 cells were seeded in 24-well plates at a density of 4 × 10^4 cells per well. Once the cells had fully adhered to the substrate, mCherry-EGFP-LC3 adenovirus infection was performed using the half-volume infection method. Specifically, all cells, including controls, were first incubated with 250 μl of fresh complete medium. The appropriate amount of virus was then added to each well, and infection proceeded for 4 h. Afterward, the volume was replenished to 500 μl of total culture volume. The infection was prolonged for 12 h. Subsequently, the virus-containing culture medium was aspirated and replaced with a fresh, complete culture medium, and incubation was resumed. Following 48 h of infection, the cells were divided into normal-growing cells (control group) and HG-induced MIN6 cells. After 48 h of puerarin treatment, subsequent experiments were conducted. The culture fluid was aspirated and washed once with PBS, a fresh complete culture medium was added, and observation was conducted using a fluorescence microscope.

2.11. Quantitative real-time PCR (RT-qPCR) detection

MIN6 cells were seeded in 6-well plates at a density of 3 × 10^5 cells per well. After the cells had fully adhered, they were divided into normal-growing cells (control) and HG-induced MIN6 cells. Following 48 h of puerarin treatment, the cell cultures were discarded. Cellular RNA was isolated using an RNA extraction kit (Tiangen Biotech, Beijing, China), and its concentration was quantified. Subsequently, cDNA was synthesized using the M5 Sprint qPCR RT kit reagent (Mei5 Biotechnology, Beijing, China), followed by cDNA amplification employing a 2x M5 HiPer SYBR Premix EsTaq reagent. β-actin was used as an internal reference. The primer sequences are shown in Table 1. Relative expression data were analyzed using the $2^{-\Delta\Delta Ct}$ method.

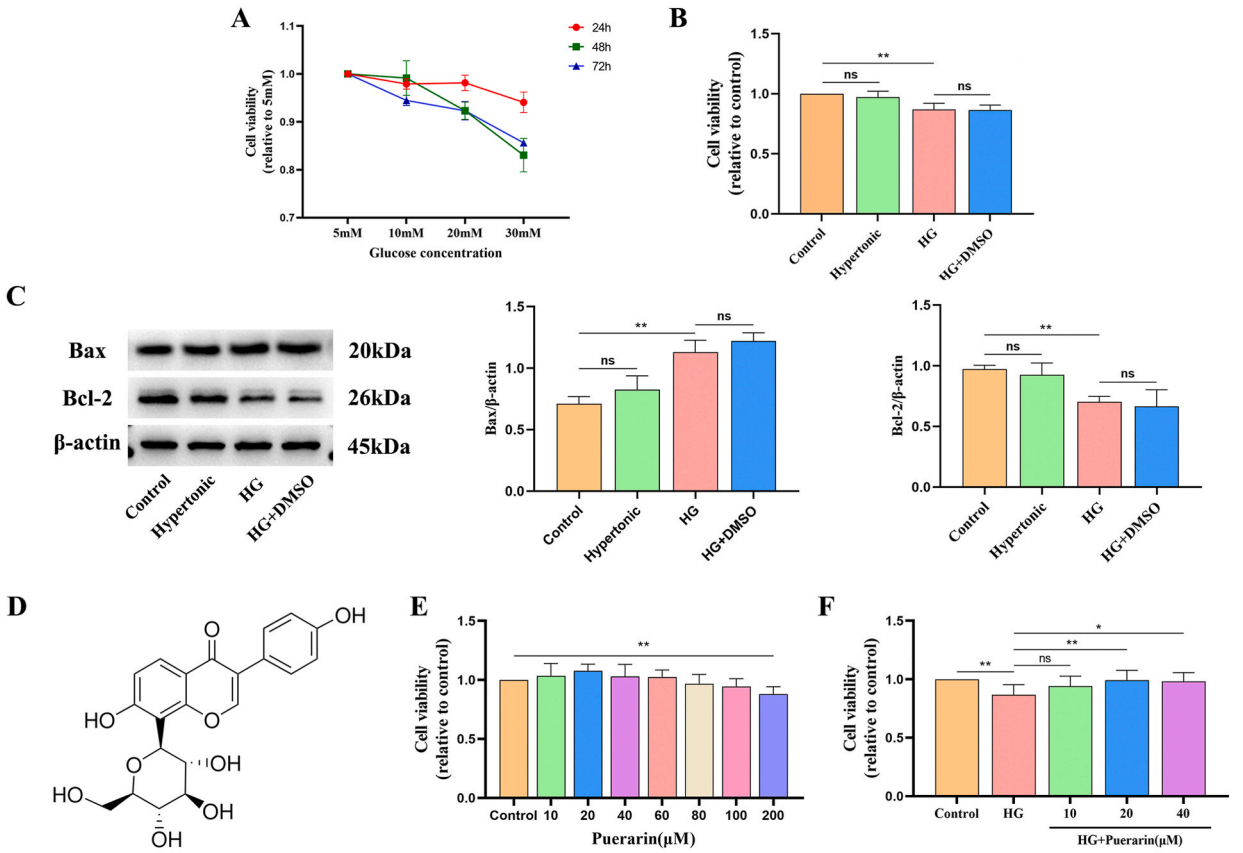

Fig. 1. (A) MIN6 cells were exposed to different glucose concentrations for 24, 48, and 72 h to measure cell viability. (B) The effects of hypertonic conditions, high glucose (HG), and DMSO on the viability of MIN6 cells. (C) Western blot detection of Bax and Bcl-2 protein expression levels in MIN6 cells under hypertonic conditions, HG, and DMSO treatments. Uncropped gels and blots refer to Fig. S1 in supplementary material. Representative images (left) and quantitative data (right) are presented. (D) The chemical structural formula of puerarin. (E) MIN6 cells were treated with different concentrations of puerarin for 48 h to measure cell viability. (F) Effect of puerarin on the viability values of MIN6 cells under the effect of high glucose. CCK-8 results are expressed as mean ± SD (n = 6). Western blot results are expressed as mean ± SD (n = 3). $^{*}P < 0.05$, $^{**}P < 0.01$. ns: no significant difference.

2.12. Western blotting

MIN6 cells were seeded in 6-well plates at a density of 3 × 10^5 cells per well. After the cells had fully adhered, they were divided into normal-growing cells (control) and HG-induced MIN6 cells. After 48 h of puerarin treatment, the cell cultures were discarded. A lysis solution (containing 1 % PMSF and 1 % phosphatase inhibitor) was added and incubated for 10 min. The lysate was then collected and centrifuged at 12,000 rpm for 10 min. The supernatant was carefully collected, and the protein concentration was determined using a bicinchoninic acid (BCA) protein assay kit. Proteins were resolved via sodium dodecyl sulfate-polyacrylamide gel electrophoresis (SDS-PAGE) and transferred onto polyvinylidene fluoride membranes (PVDF). The membranes were blocked with 1 × protein-free rapid blocking buffer for 1 h, followed by overnight incubation with primary antibodies at 4 °C, included Bax (CST, 14796), Bcl-2 (Abcam, ab196495), Cytochrome *c* (CST, 11940), Caspase-3 (Abcam, ab79123), Caspase-9 (Abcam, ab184786), LC3B (Abcam, ab192890), Beclin-1 (Abcam, ab207612), SQSTM1/p62 (CST, 23214), PINK1 (Affinity, 85h3726), p-PINK1 (Affinity, 77h3625), Parkin (Affinity, 13v0541), p-Parkin (Affinity, 77h3625), and β-actin (CST, 4967) antibodies. Afterward, the membranes were washed with TBST and incubated with HRP-conjugated Affinipure Goat Anti-Rabbit IgG (1:5000, Sanying Biology Technology, Wuhan, China) for 1 h. After rewashing the membrane with TBST, the protein bands were visualized using an electrochemiluminescence (ECL) kit (Biosharp, Shanghai, China) and a ChemiDoc XRS + gel imaging system. The grayscale values of the bands were analyzed using ImageJ software. Three protein strip images were imported for each group, and the relevant regions were boxed and analyzed to obtain the grayscale values. Furthermore, the same experimental approach was employed to evaluate the effects of hypertonicity and DMSO on cellular protein expression. MIN6 cells were seeded in 6-well plates at a density of 3 × 10^5 cells per well. Once the cells had fully adhered to the plate, they were categorized into four groups: normal-growing MIN6 cells (control), MIN6 cells in a hypertonic environment, HG-induced MIN6 cells, and HG-induced DMSO-treated MIN6 cells. The impact on cell protein expression was assessed after 48 h following the aforementioned Western blotting experimental procedure.

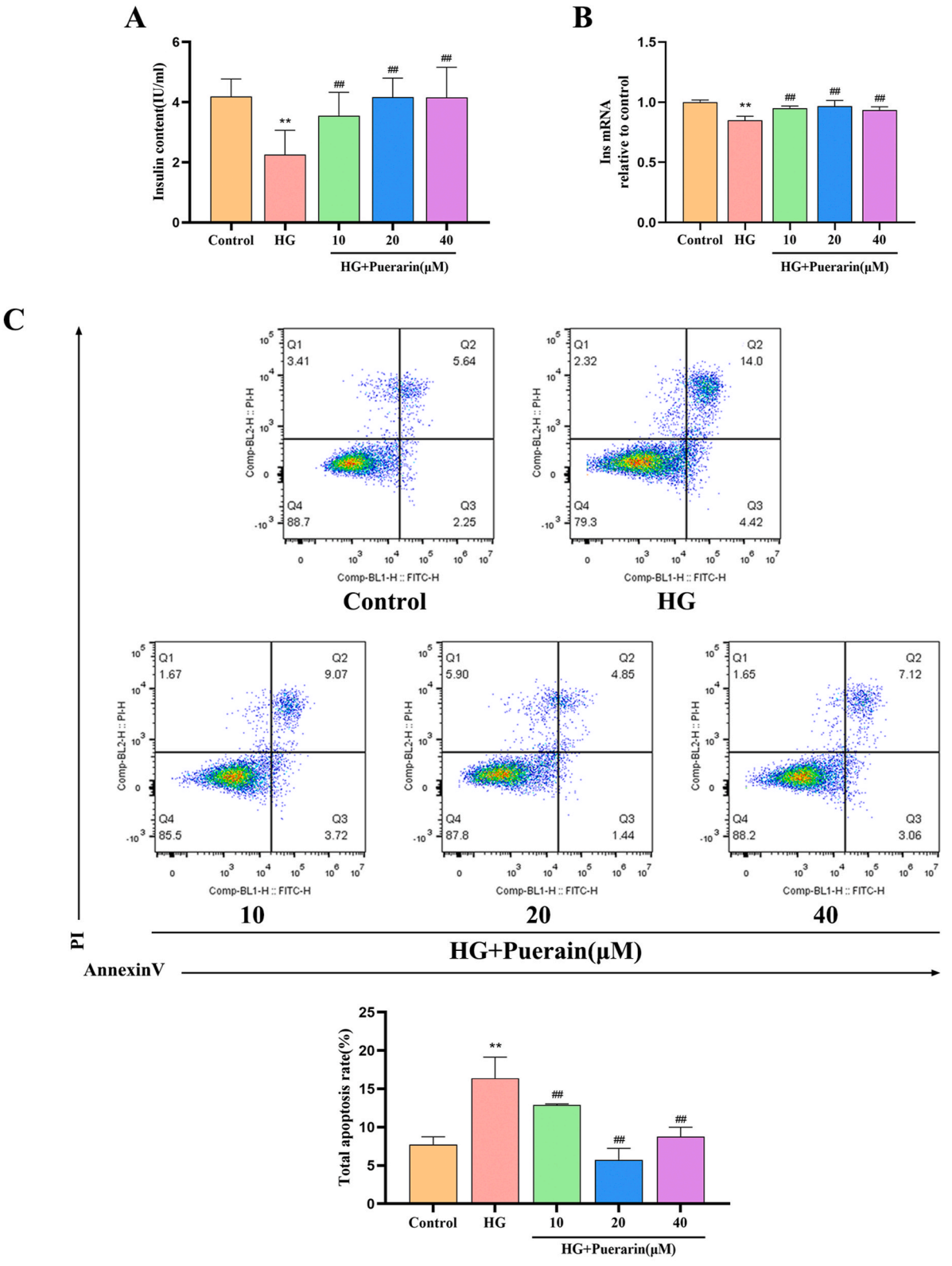

(caption on next page)

Fig. 2. (A) ELISA was applied to detect insulin secretion in MIN6 cells. (B) RT-qPCR was performed to detect the expression level of insulin mRNA (Ins mRNA) in MIN6 cells. (C) The apoptosis rate of MIN6 cells was detected by flow cytometry. ELISA results are expressed as mean ± SD (n = 6). RT-qPCR and flow cytometry results are expressed as mean ± SD (n = 3). Compared with the control group, $^{**}P < 0.01$. Compared with the HG group, $^{\#\#}P < 0.01$.

2.13. Statistical analysis

Data analysis for each group was conducted using SPSS 21.0, and graphs were generated using GraphPad Prism 9. Results are expressed as the mean ± standard deviation (SD) of at least three independent experiments. After testing for normality, data were analyzed by one-way analysis of variance (ANOVA) followed by pairwise comparisons using the LSD method. A P-value of <0.05 was considered statistically significant.

3. Results

3.1. Effect of different concentrations of glucose and time on the viability values of MIN6 cells

Following the exposure of MIN6 cells to varying glucose concentrations (5, 10, 20, and 30 mM) for 24 h, no significant alterations in cell viability were observed, with all groups maintaining high viability levels. However, after 48 and 72 h of treatment, a comparison with the 5 mM glucose group revealed that 20 mM and 30 mM glucose concentrations induced a decreasing trend in cell viability. Among these, the 30 mM glucose concentration exhibited the most pronounced decrease in cell viability (Fig. 1A). Consequently, a glucose concentration of 30 mM for 48 h was selected as the HG injury model condition for MIN6 cells.

3.2. Effects of hypertonic environment and DMSO on viability values and Bax and Bcl-2 protein expression in MIN6 cells

In this study, we created an osmotic environment equivalent to 30 mM glucose concentration by supplementing with mannitol (25 mM) to investigate the influence of osmotic pressure on cellular responses [15]. Additionally, to mitigate the impact of DMSO (40 μM) on HG-induced damage in MIN6 cells, a HG + DMSO group was included as a control alongside the HG group. Initially, the impacts of hypertonicity and DMSO on cell viability were assessed using the CCK-8 assay. Relative to the control group, the hypertonic group exhibited no significant alteration in cell viability, whereas the HG group displayed a notable decrease in cell viability ($P < 0.01$). Conversely, the HG + DMSO group showed no significant difference in cell viability compared to the HG group (Fig. 1B). Subsequently, we investigated the impact of hypertonicity and DMSO on the apoptotic protein Bax and the anti-apoptotic protein Bcl-2 via Western blot analysis. Relative to the control group, the hypertonic group exhibited no significant alterations in Bax and Bcl-2 protein expression. Conversely, the HG group displayed a significant increase in Bax protein expression ($P < 0.01$) and a significant decrease in Bcl-2 protein expression ($P < 0.01$). Notably, there were no significant changes in either Bax or Bcl-2 protein expression in the HG + DMSO group compared to the HG group (Fig. 1C). These findings indicate that apoptosis is induced in MIN6 cells at a glucose concentration of 30 mM, consistent with the observations in Fig. 1B. Furthermore, these data results preclude the influence of hyperosmotic environments on MIN6 cell damage and the impact of DMSO on puerarin administration.

3.3. Puerarin promotes HG-induced increase in MIN6 cell viability values

The chemical structure of puerarin is depicted in Fig. 1D. MIN6 cells were incubated under normal culture conditions (5 mM glucose concentration) for 48 h. Treatment with 200 μM of puerarin resulted in a significant decrease in cell viability ($P < 0.01$), while no significant changes were observed with other concentrations (Fig. 1E). Following 48 h of HG incubation (Fig. 1A), the viability of MIN6 cells markedly decreased compared to the 5 mM glucose concentration. However, co-culture treatment with 20 and 40 μM of puerarin under HG conditions significantly recovered cell viability ($P < 0.05$, $P < 0.01$; Fig. 1F). These findings suggest that puerarin may protect against HG-induced damage in MIN6 cells.

3.4. Puerarin promotes HG-induced insulin gene expression and insulin secretion in MIN6 cells

The findings revealed a significant downregulation of insulin mRNA expression and secretion in MIN6 cells following HG treatment ($P < 0.01$). Conversely, intervention with puerarin (10, 20, and 40 μM) significantly improved both insulin mRNA expression and insulin secretion ($P < 0.01$; Fig. 2A and B). These results suggest that puerarin can enhance insulin mRNA expression and secretion in HG-induced MIN6 cells.

3.5. Puerarin attenuates HG-induced apoptosis in MIN6 cells

Illustrated in Fig. 2C, treatment with HG significantly increased the apoptosis rate of MIN6 cells ($P < 0.01$), a trend markedly mitigated by puerarin intervention ($P < 0.01$). These findings suggest that puerarin can attenuate HG-induced apoptosis of MIN6 cells, thereby exerting a protective effect.

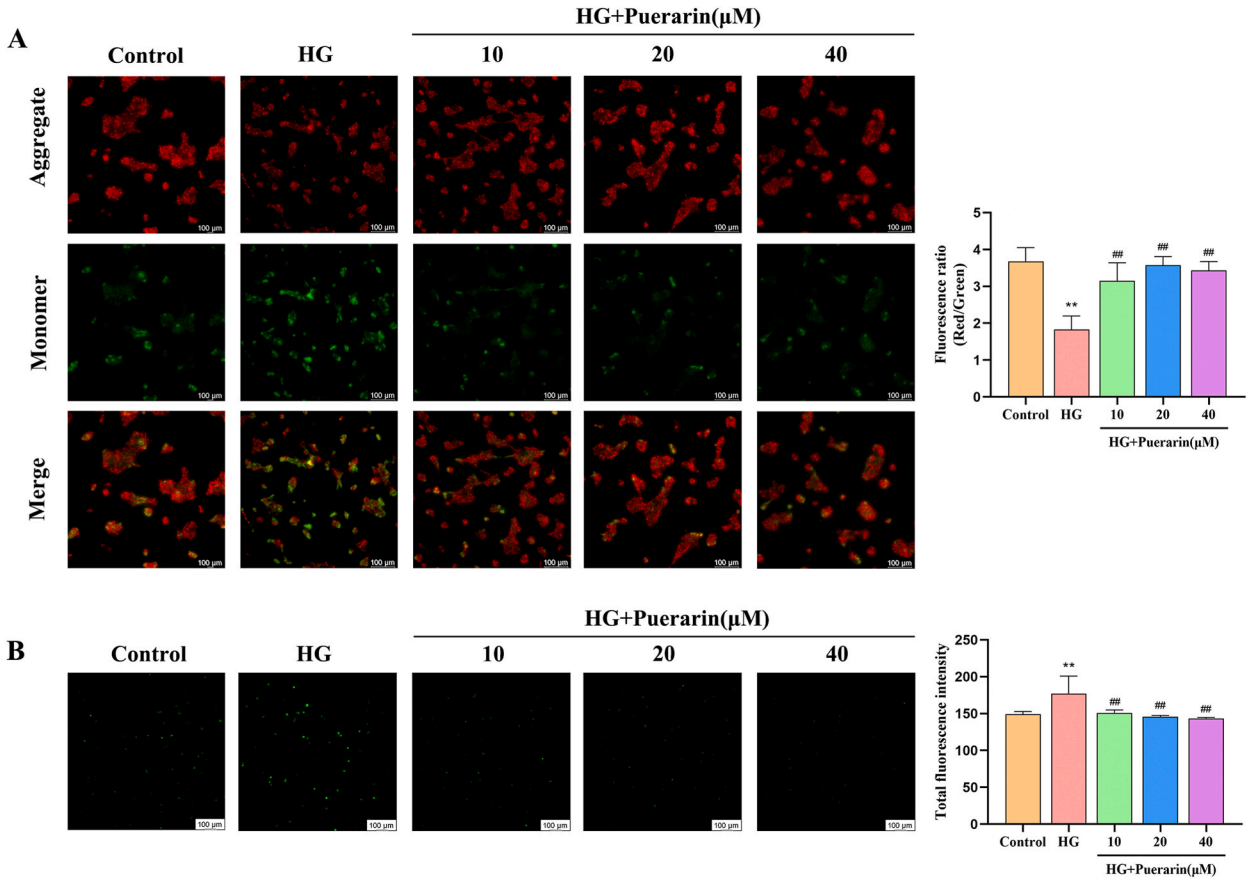

Fig. 3. (A) JC-1 detects mitochondrial membrane potential changes in MIN6 cells. (B) DCFH-DA fluorescent probe to detect ROS production in MIN6 cells. The results are expressed as mean ± SD (n = 3). Compared with the control group, $^{**}P < 0.01$. Compared with the HG group, $^{\#\#}P < 0.01$.

3.6. Puerarin attenuates HG-induced mitochondrial damage and high ROS production in MIN6 cells

Apoptosis is frequently accompanied by mitochondrial damage, and a reduction in mitochondrial membrane potential (MMP) indicates mitochondrial damage [16]. The results depicted in Fig. 3A indicate that HG treatment markedly reduced the MMP of MIN6 cells ($P < 0.01$), a trend reversed by puerarin intervention ($P < 0.01$). Additionally, mitochondria are the primary organelles for ROS generation, and excessive ROS production can exacerbate mitochondrial damage. As depicted in Fig. 3B, HG treatment markedly increased ROS production in MIN6 cells ($P < 0.01$), a trend markedly alleviated by puerarin intervention ($P < 0.01$). These findings suggest that puerarin mitigates HG-induced mitochondrial damage and excessive ROS production in MIN6 cells.

3.7. Puerarin inhibits HG-induced activation of Bax/Bcl-2/caspase-3 signalling pathway in MIN6 cells

The mitochondrial apoptotic pathway plays a crucial role in inducing apoptosis. The results depicted in Fig. 4A demonstrate that treatment with HG significantly upregulated the mRNA expression of Bax, Cyt-c, Caspase 3, and Caspase 9 ($P < 0.01$) while concurrently downregulating Bcl-2 mRNA expression ($P < 0.01$) in MIN6 cells. Notably, these effects were efficiently attenuated by puerarin intervention. Consistent with the mRNA findings, the results depicted in Fig. 4B reveal that HG treatment significantly increased the protein expression levels of Bax, Cyt-c, Cleaved Caspase 3, and Cleaved Caspase 9 ($P < 0.01$) while concurrently decreasing Bcl-2 protein expression ($P < 0.05$) in MIN6 cells. Notably, these effects were efficiently mitigated by puerarin intervention. These findings suggest that puerarin effectively inhibits the activation of the Bax/Bcl-2/Caspase-3 signaling pathway, thereby attenuating apoptosis in HG-induced MIN6 cells.

3.8. Puerarin promotes the fusion of mitochondria and lysosomes within HG-induced autophagosomes of MIN6 cells

The fusion between mitochondria and lysosomes serves as an indicator of the modulation of mitochondrial autophagy function. The degree of correlation between mitochondria and lysosomes can be assessed by calculating the fluorescence co-localization correlation

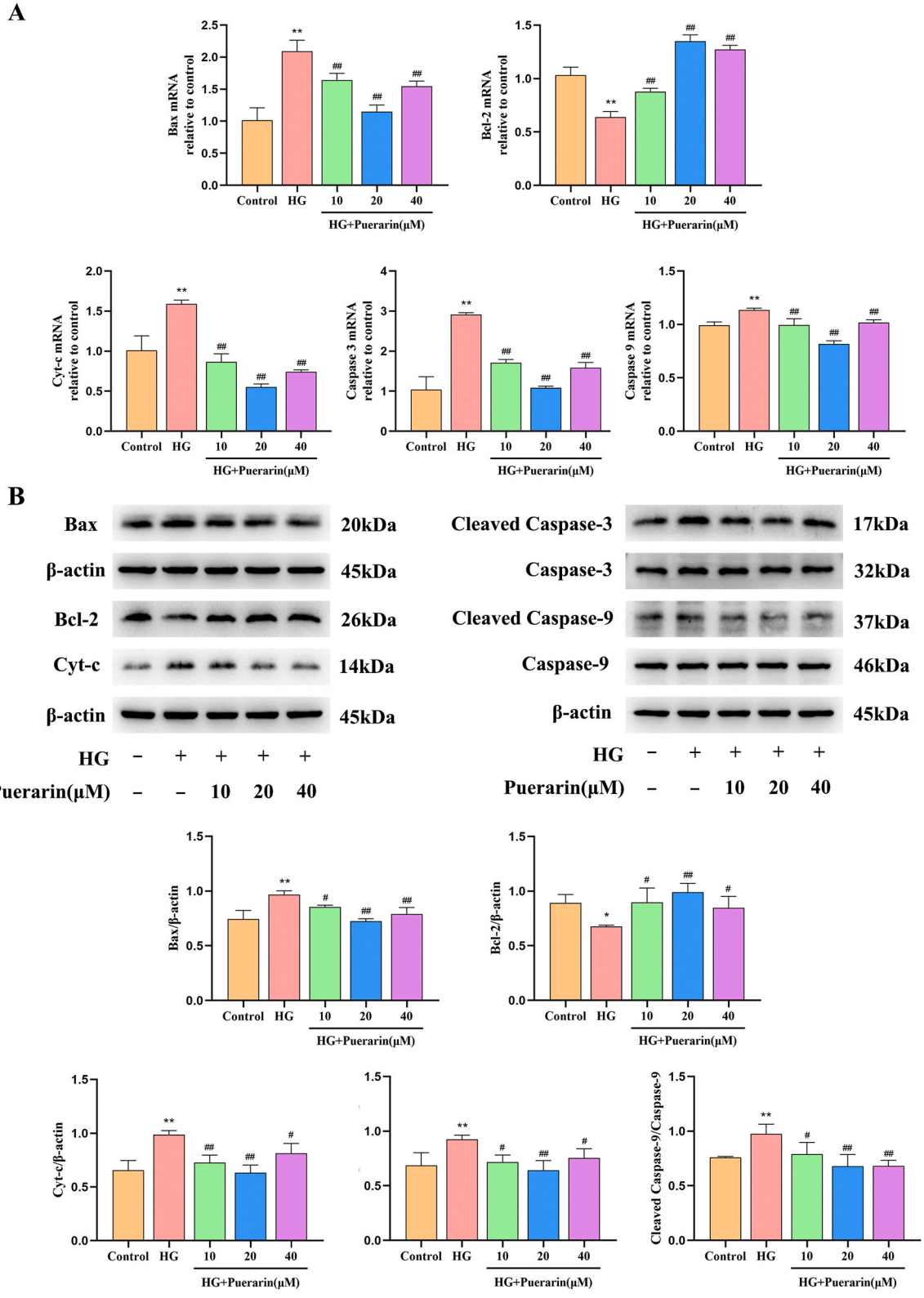

(caption on next page)

Fig. 4. (A) RT-qPCR detection of Bax, Bcl-2, Cyt-c, Caspase 3 and Caspase 9 mRNA expression levels in MIN6 cells. (B) Western blot was used to detect the protein expression levels of Bax, Bcl-2, Cyt-c, Cleaved Caspase 3 and Cleaved Caspase 9 in MIN6 cells. The representative images (above) and quantitative data (below) are presented. Uncropped gels and blots refer to Fig. S2 in supplementary material. The results are expressed as mean ± SD (n = 3). Compared with the control group, $^{*}P < 0.05$, $^{**}P < 0.01$. Compared with the HG group, $^{\#}P < 0.05$, $^{\#\#}P < 0.01$.

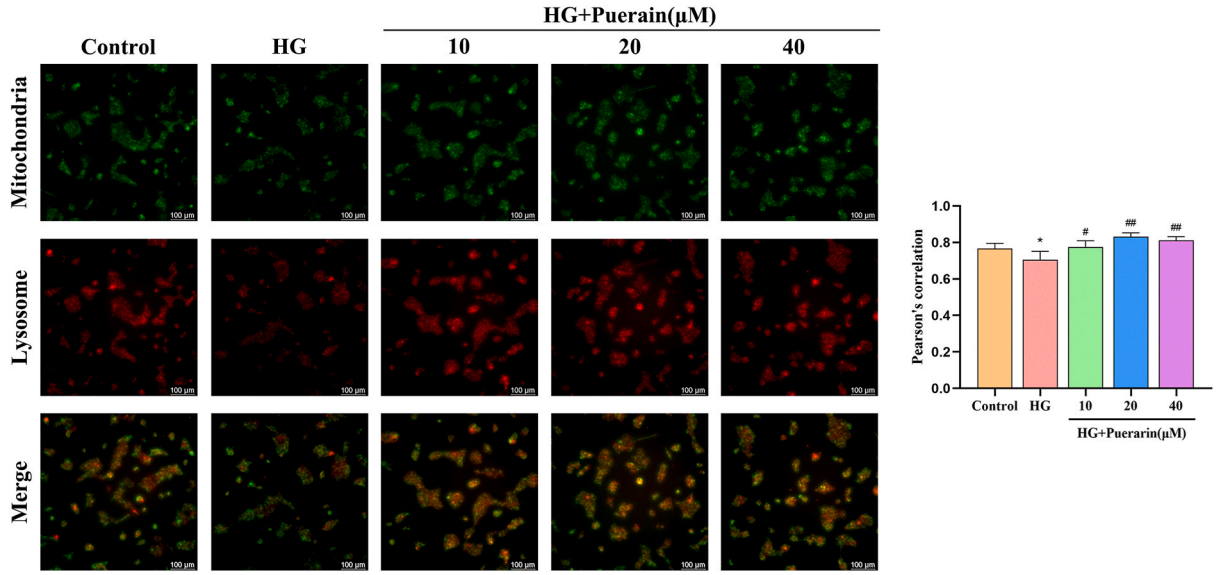

Fig. 5. Co-localization of Mito-Tracker Green and Lyso-Tracker Red shows the level of mitochondrial and lysosomal fusion in MIN6 cells. The results are expressed as mean ± SD (n = 3). Compared with the control group, $^{*}P < 0.05$. Compared with the HG group, $^{\#}P < 0.05$, $^{\#\#}P < 0.01$.

coefficient, specifically Pearson's coefficient. A value approaching 1 signifies a robust linear relationship between these organelles. In Fig. 5, it is evident that the merging of green mitochondria and red lysosomes resulted in the formation of yellow fluorescence. Notably, HG treatment decreased the fusion extent between mitochondria and lysosomes in MIN6 cells ($P < 0.05$), reducing yellow fluorescence and inhibiting mitochondrial autophagy. Conversely, puerarin intervention significantly augmented the fusion of mitochondria and lysosomes ($P < 0.05$, $P < 0.01$), increasing yellow fluorescence and enhancing mitochondrial autophagy. These findings suggest that puerarin facilitates HG-induced fusion between mitochondria and lysosomes, thereby augmenting mitochondrial autophagy in MIN6 cells.

3.9. Puerarin promotes HG-induced fusion of autophagosomes with lysosomes in MIN6 cells

To probe the alterations in LC3 protein expression within MIN6 cells under an HG environment, we subjected the cells to infection with mCherry-EGFP-LC3 adenovirus as part of this study in order to assess the suitable multiplicity of infection (MOI). It was observed that with MOI = 30, the fluorescence intensity significantly increased compared to MOI = 10. However, at MOI = 100, while the fluorescence intensity increased further, there was a significant decrease in cell number, indicating cytotoxicity (Fig. 6A). Hence, an MOI of 30 was deemed appropriate. In the mCherry-EGFP-LC3 dual fluorescence labelling system, changes in EGFP (green) and mCherry (red) fluorescence can indicate the fusion of autophagosomes and lysosomes. Compared with the control group, green fluorescence remained unchanged, while red fluorescence diminished following HG treatment, suggesting that the fusion of autophagosomes and lysosomes was impeded, resulting in decreased autophagic function. After puerarin intervention, red fluorescence intensified, and green fluorescence diminished due to quenching in the acidic lysosomal environment, indicating that autophagosomes fused with lysosomes, thereby enhancing autophagic function (Fig. 6B). The results demonstrated that puerarin facilitates the fusion of autophagosomes with lysosomes induced by HG in MIN6 cells.

3.10. Puerarin enhances PINK1/Parkin-mediated mitochondrial autophagy in HG-induced MIN6 cells

Mitochondrial autophagy is a crucial and fundamental process for maintaining cellular homeostasis, which requires initiation through specific mechanisms [8]. The PINK1/Parkin pathway represents the principal route of mitochondrial autophagy. Fig. 7A revealed that HG treatment markedly reduced the mRNA expression of PINK1, Parkin, Beclin-1, and LC3II ($P < 0.01$) while increasing p62 mRNA expression ($P < 0.01$) in MIN6 cells. These effects were effectively reversed by puerarin intervention. Similarly, the protein-level findings depicted in Fig. 7B demonstrated that HG treatment significantly decreased the expression of p-PINK1, p-Parkin, Beclin-1, and the LC3II/LC3I ratio ($P < 0.05$, $P < 0.01$), while increasing p62 protein expression ($P < 0.05$, $P < 0.01$) in MIN6 cells.

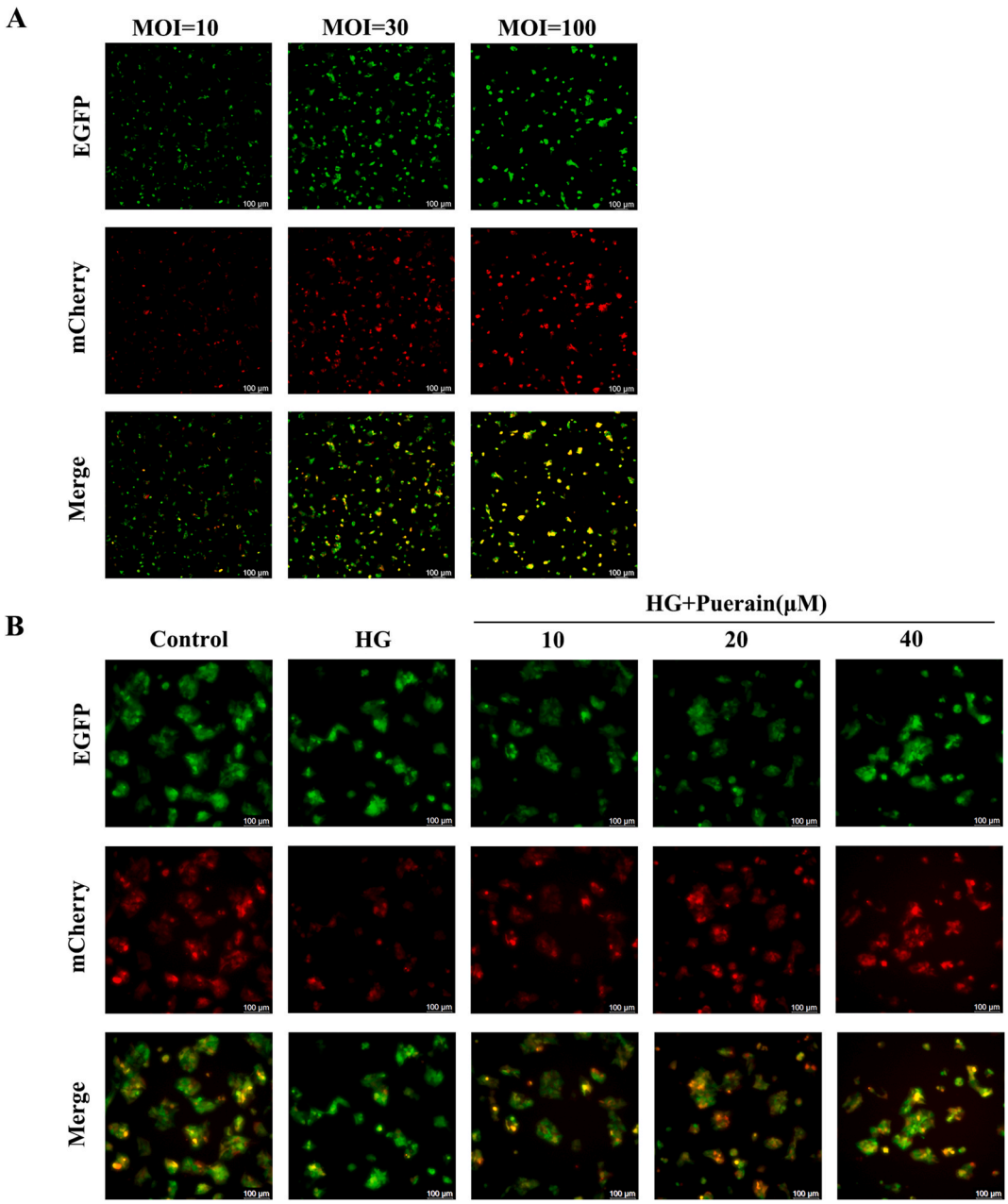

Fig. 6. (A) Pre-experimental screening of suitable multiplicity of infection (MOI). (B) mCherry-EGFP-LC3 adenovirus infection shows fusion levels of autophagosomes and lysosomes in MIN6 cells.

These alterations were efficiently reversed by puerarin intervention. These findings suggest that puerarin enhances HG-induced mitochondrial autophagy mediated by the PINK1/Parkin pathway in MIN6 cells, thereby exerting a protective effect.

4. Discussion

T2DM is a chronic metabolic disorder characterized by progressively elevated blood glucose levels over time [17]. β-cells are distinctive endocrine cells. Chronic exposure to hyperglycemia often leads to a progressive decline in β-cell function, resulting in impaired insulin action and secretion [18]. Furthermore, a potential mechanism for the progressive decrease in β-cell mass in patients with T2DM has been identified as an increase in β-cell apoptosis [19]. Increased β-cell apoptosis and reduced β-cell numbers are primary manifestations of pancreatic β-cell dysfunction. β-cell apoptosis impairs the insulin signaling pathway, accelerating cellular dysfunction and decreasing insulin secretion [20]. Consequently, β-cell dysfunction is considered crucial in T2DM pathogenesis [21],

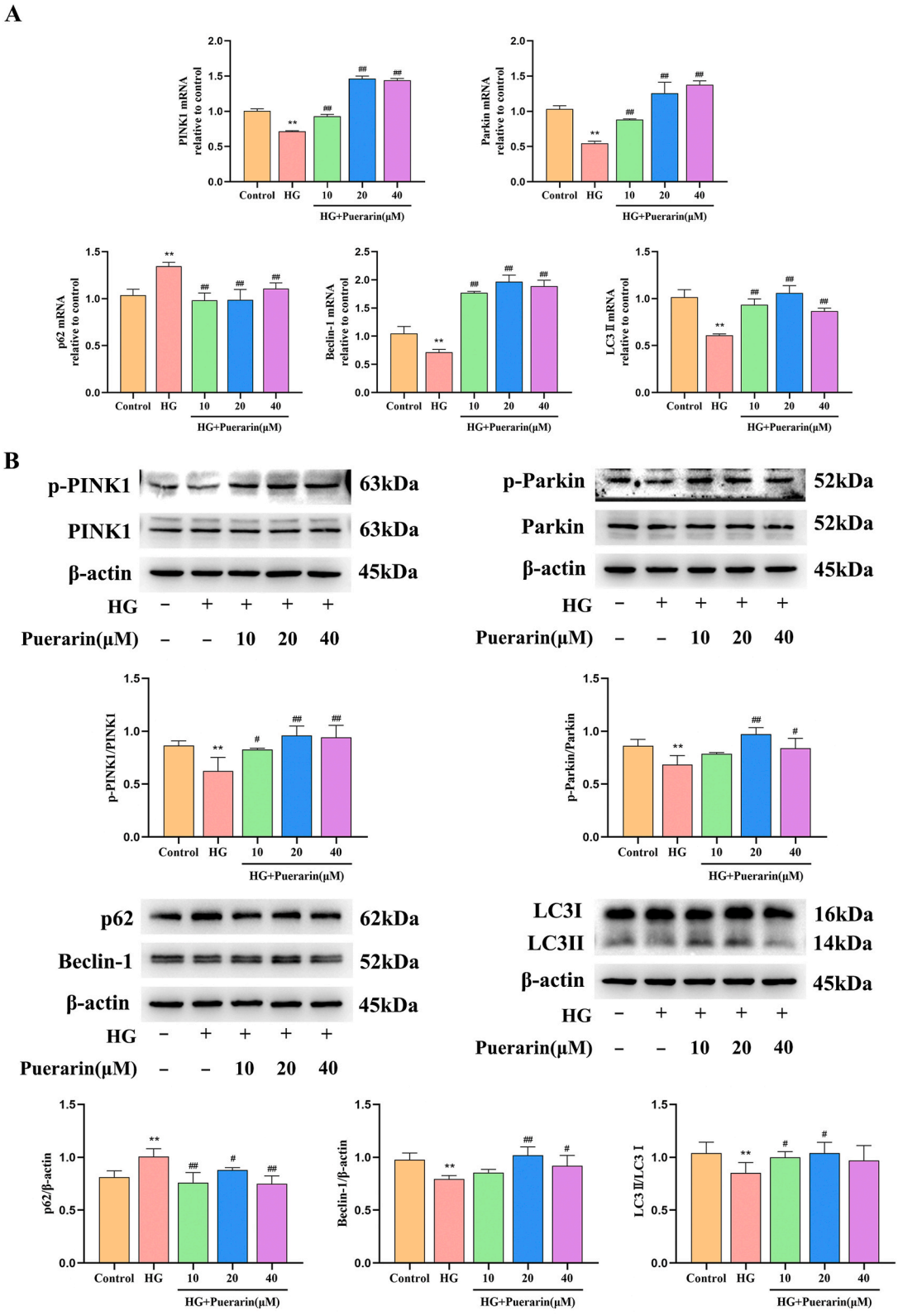

(caption on next page)

Fig. 7. (A) RT-qPCR detection of PINK1, Parkin, Beclin-1, p62 and LC3II mRNA expression levels in MIN6 cells. (B) Western blot detection of p-PINK1, p-Parkin, Beclin-1, p62 and LC3II/LC3I protein expression levels in MIN6 cells. The representative images (above) and quantitative data (below) are presented. Uncropped gels and blots refer to Fig. S3 in supplementary material. The results are expressed as mean ± SD (n = 3). Compared with the control group, $^{**}P < 0.01$. Compared with the HG group, $^{\#}P < 0.05$, $^{\#\#}P < 0.01$.

and strategies aimed at protecting β-cells from injury and apoptosis are deemed beneficial. The MIN6 cell line, possessing characteristics of pancreatic islet β-cells and exhibiting glucose-stimulated insulin secretion, is derived from mouse pancreatic islets [22]. In this study, we replicated the *in vivo* environment of pancreatic β-cells in T2DM mice by subjecting MIN6 cells to prolonged exposure to HG levels to explore puerarin's protective effects against pancreatic β-cell injury under HG conditions. The study findings demonstrated that puerarin attenuated MIN6 cell injury and enhanced insulin secretion in an HG environment, with its mechanism of action being associated with PINK1/Parkin-mediated mitochondrial autophagy.

Oxidative stress represents a primary mechanism underlying pancreatic β-cell dysfunction, exacerbated by the scarcity of antioxidant enzymes within these cells [23]. ROS constitute a collection of oxygen-derived reactive molecules and free radicals primarily originating from mitochondria, serving as the principal organelle targets for ROS-mediated damage [24]. The excessive buildup of ROS precipitates inevitable repercussions on mitochondrial respiration, augmenting mitochondrial membrane permeability and culminating in mitochondrial dysfunction and cellular demise [25]. Previous studies have demonstrated that puerarin possesses antioxidant properties and can inhibit the onset of diseases induced by ROS [26,27]. In this investigation, we have illustrated that puerarin markedly enhances cell viability, diminishes ROS generation, and reinstates mitochondrial membrane potential under hyperglycemic conditions. Apoptosis is a regulated process of programmed cell death initiated by exogenous or endogenous factors and governed by a diverse array of genes [28]. Numerous studies have demonstrated that ROS can engage with mitochondria via intrinsic pathways, thereby orchestrating the mitochondrial apoptotic pathway to instigate apoptosis [29,30]. Within the intricate orchestration of apoptosis, the Bcl-2 family proteins, encompassing the pro-apoptotic factor Bax and the anti-apoptotic factor Bcl-2, assume pivotal roles [31,32]. Typically, Bax interacts with Bcl-2-related proteins, thereby preserving a relatively stable protein expression level [33]. Upon induction of the mitochondrial apoptotic pathway, the Bax protein undergoes a conformational alteration, translocating from the cytoplasm to the outer mitochondrial membrane [34]. This phenomenon concomitates with the opening of the mitochondrial permeability transition pore (MPTP), culminating in the depolarization of mitochondrial membrane potential and the augmentation of mitochondrial membrane permeability [35,36]. The pro-apoptotic factor Cytochrome *c* (Cyt-c), initially sequestered within mitochondria, is released into the cytoplasm, where it complexes with apoptotic protease-activating factor-1 (Apaf-1), initiating a cascade of events culminating in the activation of Caspase-9, which subsequently activates the downstream effector enzyme Caspase-3, ultimately culminating in apoptotic cell death [37,38]. In this study, we observed that puerarin intervention significantly reduced apoptosis of MIN6 cells under HG conditions, as assessed by flow cytometry analysis. Furthermore, we conducted a comprehensive investigation into the involvement of the mitochondrial apoptotic pathway using Western blot and RT-qPCR techniques. Data analysis revealed activation of the mitochondrial apoptotic pathway in MIN6 cells under HG conditions, which was reversed by puerarin treatment. Our findings indicate that puerarin mitigates ROS generation, thereby reducing apoptosis via the mitochondrial apoptotic pathway, safeguarding β-cells against apoptotic insults, and preserving β-cell function integrity. This discovery offers a novel theoretical framework for utilizing puerarin in managing T2DM and associated disorders.

Autophagy is a dual-purpose cytoprotective process and a safeguarding mechanism for cellular survival, primarily achieved by removing toxic proteins and damaged organelles [39]. Research conducted by Zummo et al. [40] has demonstrated that compromised autophagic flux can contribute to β-cell mass reduction in individuals with T2DM. In contrast, reinstatement of autophagic function enhances β-cell viability. Thus, maintaining normal levels of autophagy is essential for preserving intracellular homeostasis and modulating cell function and survival. In recent years, there has been a growing emphasis on investigating the interplay between mitochondrial autophagy and apoptosis. Numerous studies have demonstrated a close correlation between the ROS-mediated mitochondrial apoptotic pathway and dysfunction in mitochondrial autophagy [41,42]. Mitochondrial autophagy, a specialized form of autophagy, selectively eliminates damaged or malfunctioning mitochondria, mitigates mitochondrial overaccumulation, and sustains mitochondrial mass and energy metabolism [43]. PINK1/Parkin constitutes an upstream pathway governing the regulation of mitochondrial autophagy. Excessive ROS production induces a decline in mitochondrial membrane potential, thereby facilitating the recruitment of PINK1 to the outer mitochondrial membrane, triggering Parkin activation and instigating mitochondrial autophagy [44]. In this investigation, the protein levels of p-PINK1/PINK1 and p-Parkin/Parkin were notably diminished in MIN6 cells exposed to a HG environment, while p-PINK1/PINK1 and p-Parkin/Parkin levels experienced a marked increase following puerarin intervention. These findings suggest that puerarin exerts a pronounced ameliorative effect on mitochondrial autophagy in HG-injured MIN6 cells. Furthermore, ROS-induced damage to mitochondria triggers the accumulation of p62 protein on the mitochondrial surface, facilitating its binding to LC3 protein and promoting the formation of mitochondrial autophagosomes [45]. A study demonstrated that HG treatment suppressed mitochondrial autophagy by reducing the LC3II/LC3I ratio and increasing p62 mRNA expression in human gingival epithelial cells [46]. Consequently, we investigated the expression of proteins related to mitochondrial autophagy. The p62 protein functions as a junction protein in mitochondrial autophagy, facilitating the linkage of ubiquitinated substrates to LC3 proteins and promoting the degradation of ubiquitinated proteins within autophagosomes; additionally, it serves as an indicator of autophagic flux [47]. Its protein levels exhibited a negative correlation with the extent of mitochondrial autophagy. In the process of mitochondrial autophagy, damaged mitochondria are enveloped by the endoplasmic reticulum membrane to generate autophagosomes, with the LC3 protein playing a pivotal role in their formation [45]. The LC3 protein exists in two forms: LC3 I, found in the cytoplasm, and LC3 II, present in both the inner and outer membranes of mitochondrial autophagosomes [48]. The conversion of LC3 I to LC3 II

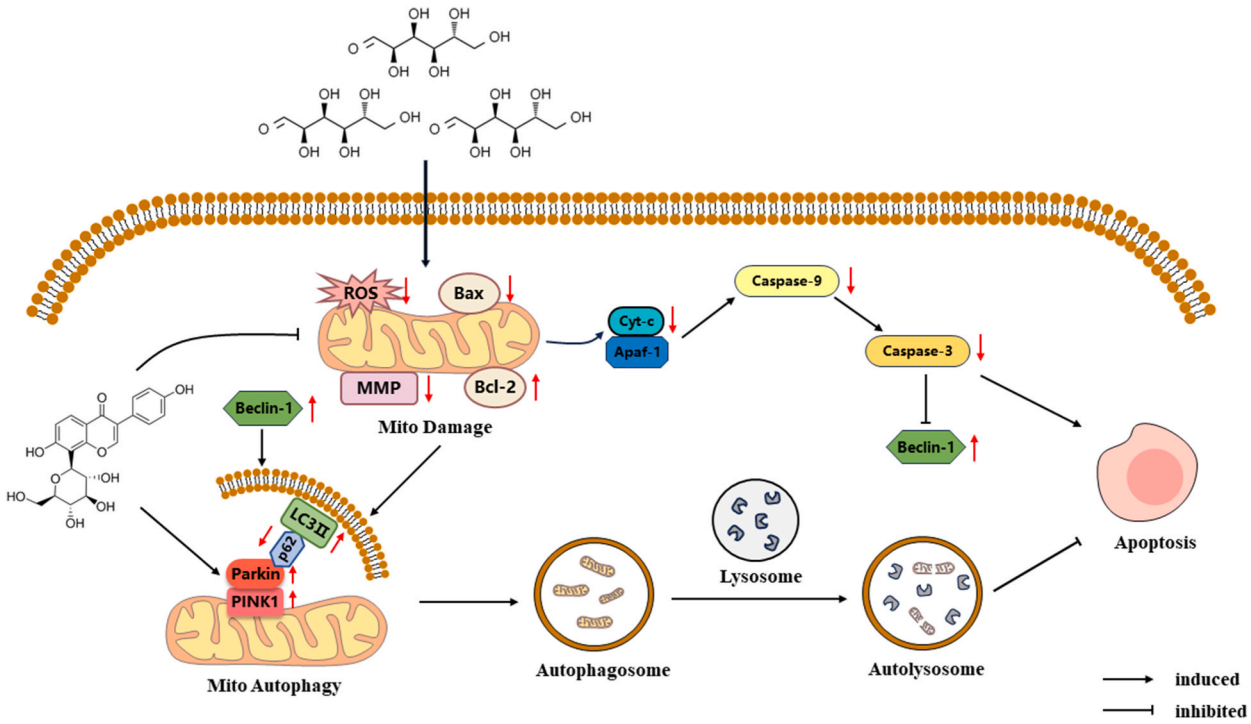

Fig. 8. Schematic illustration of puerarin inhibiting mitochondrial apoptosis under high glucose (HG) by promoting PINK1/Parkin-mediated mitochondrial autophagy.

promotes the fusion of mitochondrial autophagosomes with lysosomes [48]. Consequently, the LC3 II to LC3 I ratio is commonly employed to evaluate the extent of mitochondrial autophagy. Beclin-1, a member of the autophagy-related protein family, interacts with LC3 proteins to initiate mitochondrial autophagy. Additionally, caspase 3 has been implicated in inhibiting mitochondrial autophagy and promoting apoptosis through Beclin-1 cleavage [49]. This study observed a significant down-regulation of LC3II/LC3I and Beclin-1 mRNA and protein expression, alongside a significant up-regulation of p62 mRNA and protein expression in MIN6 cells exposed to a HG environment, a trend effectively counteracted by puerarin intervention. Moreover, the outcomes of mCherry-EGFP-LC3 adenovirus infection provide additional evidence suggesting that puerarin enhances the fusion of autophagosomes with autophagic lysosomes, thus promoting mitochondrial autophagy. In conclusion, our findings indicate that puerarin facilitates PINK1/Parkin-mediated mitochondrial autophagy.

This study presents a novel theoretical framework for safeguarding pancreatic β-cells against glucotoxic damage through puerarin intervention. Nevertheless, due to the complexity of the molecular mechanism underlying mitochondrial autophagy, characterized by the existence of numerous different mechanisms, and our exclusive focus on the PINK1/Parkin-mediated mitochondrial autophagy pathway, there are limitations that will be addressed in future studies. Additionally, the investigation of pancreatic islet inflammation induced by islet macrophage infiltration is garnering attention, which may represent another pivotal factor contributing to β-cell injury. Consequently, the subsequent experimental approach involved co-culturing MIN6 cells with macrophages to explore the potential of puerarin in shielding β-cells from inflammatory factors secreted by macrophages.

5. Conclusion

The present investigation elucidated that puerarin possesses the capability to impede the activation of the mitochondrial apoptotic pathway and mitigate apoptosis by attenuating the production of ROS while fostering PINK1/Parkin-mediated mitochondrial autophagy in MIN6 cells subjected to a HG environment (Fig. 8). This outcome serves to enhance our understanding of the mechanistic actions of puerarin in ameliorating T2DM and furnishes a theoretical foundation for the prospective development of puerarin-based pharmaceuticals aimed at improving T2DM.

Disclosure statement

No potential conflict of interest was reported by the authors.

Funding

This study received support from the following funding sources: the National Key Research and Development Program of China (2017YFC1702902, China), the School-level Science and Technology Innovation Team Development Program of Jiangxi University of Chinese Medicine (CXTD22007, China), the Key Project of the Natural Science Foundation of Jiangxi Province (20232ACB206058, 20232ACB206064, China), and the National Natural Science Foundation of China (82360785, China).

Data availability statement

Data included in article/supp. material/referenced in article.

CRediT authorship contribution statement

Hongyang Zhu: Writing – original draft, Methodology, Funding acquisition, Formal analysis, Data curation, Conceptualization. **You Yu:** Writing – review & editing, Methodology, Funding acquisition, Data curation, Conceptualization. **Yuting Li:** Methodology, Data curation. **Shiyao Chang:** Methodology, Data curation. **Yuhui Liu:** Writing – review & editing, Supervision, Project administration, Funding acquisition, Conceptualization.

Declaration of competing interest

The authors declare that they have no known competing financial interests or personal relationships that could have appeared to influence the work reported in this paper.

Acknowledgements

The authors thank Jiangxi University of Chinese Medicine for providing a favorable learning environment and a high-quality research platform.

Appendix A. Supplementary data

Supplementary data to this article can be found online at https://doi.org/10.1016/j.heliyon.2024.e36176.

References

[1] Y. Chen, M. Wang, New insights of anti-hyperglycemic agents and traditional chinese medicine on gut microbiota in type 2 diabetes, Drug Des Devel Ther 152021) 4849-4863, https://doi.org/10.2147/DDDT.S334325.
[2] S. Tariq, M.R. Mirza, M.I. Choudhary, R. Sultan, M. Zafar, Prediction of type 2 diabetes at pre-diabetes stage by mass spectrometry: a preliminary study, Int. J. Pept. Res. Ther. 28 (4) (2022), https://doi.org/10.1007/s10989-022-10419-9.
[3] Q. Huang, S. Bu, Y. Yu, et al., Diazoxide prevents diabetes through inhibiting pancreatic β-cells from apoptosis via bcl-2/bax rate and p38-β mitogen-activated protein kinase, Endocrinology 148 (1) (2007) 81–91, https://doi.org/10.1210/en.2006-0738.
[4] Y. Zhang, Z. He, X. Liu, et al., Oral administration of angelica sinensis polysaccharide protects against pancreatic islets failure in type 2 diabetic mice: pancreatic β-cell apoptosis inhibition, J. Funct.Foods 54 (2019) 361–370, https://doi.org/10.1016/j.jff.2019.01.037.
[5] R.P. Robertson, J.S. Harmon, Diabetes, glucose toxicity, and oxidative stress: a case of double jeopardy for the pancreatic islet β cell, Free, Radic. Biol. Med. 41 (2) (2006) 177–184, https://doi.org/10.1016/j.freeradbiomed.2005.04.030.
[6] Y. Wang, M. Song, Q. Wang, et al., Pink1/parkin-mediated mitophagy is activated to protect against afb1-induced kidney damage in mice, Chem. Biol. Interact. 358 (2022) 109884, https://doi.org/10.1016/j.cbi.2022.109884.
[7] J. Xi, Y. Rong, Z. Zhao, et al., Scutellarin ameliorates high glucose-induced vascular endothelial cells injury by activating pink1/parkin-mediated mitophagy, J. Ethnopharmacol. 271 (2021) 113855, https://doi.org/10.1016/j.jep.2021.113855.
[8] P. Liu, C. Guo, Y. Cui, et al., Activation of pink1/parkin-mediated mitophagy protects against apoptosis in kidney damage caused by aluminum, J. Inorg. Biochem. 230 (2022) 111765, https://doi.org/10.1016/j.jinorgbio.2022.111765.
[9] Y. Yang, P. Wang, J. Guo, et al., Zinc overload induces damage to h9c2 cardiomyocyte through mitochondrial dysfunction and ros-mediated mitophagy, Cardiovasc. Toxicol. 23 (11–12) (2023) 388–405, https://doi.org/10.1007/s12012-023-09811-8.
[10] S. Shan, Z. Shen, C. Zhang, R. Kou, K. Xie, F. Song, Mitophagy protects against acetaminophen-induced acute liver injury in mice through inhibiting nlrp3 inflammasome activation, Biochem. Pharmacol. 169 (2019) 113643, https://doi.org/10.1016/j.bcp.2019.113643.
[11] Y. Ji, Y. Leng, S. Lei, et al., The mitochondria-targeted antioxidant mitoq ameliorates myocardial ischemia–reperfusion injury by enhancing pink1/parkin-mediated mitophagy in type 2 diabetic rats, Cell Stress and Chaperones 27 (4) (2022) 353–367, https://doi.org/10.1007/s12192-022-01273-1.
[12] Z. Li, S. Wang, X. Wang, et al., Pharmacodynamic interactions between puerarin and metformin in type-2 diabetic rats, Molecules 27 (21) (2022) 7197, https://doi.org/10.3390/molecules27217197.
[13] Y.L. Bai, L.L. Han, J.H. Qian, H.Z. Wang, Molecular mechanism of puerarin against diabetes and its complications, Front. Pharmacol. 12 (2021) 780419, https://doi.org/10.3389/fphar.2021.780419.
[14] Z. Li, Z. Shangguan, Y. Liu, et al., Puerarin protects pancreatic beta-cell survival via pi3k/akt signaling pathway, J. Mol. Endocrinol. 53 (1) (2014) 71–79, https://doi.org/10.1530/JME-13-0302.
[15] M. Federici, M. Hribal, L. Perego, et al., High glucose causes apoptosis in cultured human pancreatic islets of Langerhans: a potential role for regulation of specific Bcl family genes toward an apoptotic cell death program, Diabetes 50 (6) (2001) 1290–1301, https://doi.org/10.2337/diabetes.50.6.1290.
[16] M.X.X.G. Yaoyao Bian, X.W.Y.H. Zhang, Cinobufagin induces acute promyelocytic leukaemia cell apoptosis and pml-rara degradation in a caspase-dependent manner by inhibiting the β -catenin signalling pathway, Pharm. Biol. 60 (1) (2022) 1801–1811, https://doi.org/10.1080/13880209.2022.2118792.

[17] M. Abdulaziz Al Dawish, A. Alwin Robert, R. Braham, et al., Diabetes mellitus in Saudi Arabia: a review of the recent literature, Curr. Diabetes Rev. 12 (4) (2016) 359–368, https://doi.org/10.2174/1573399811666150724095130.
[18] G.C. Weir, Glucolipotoxicity, b-cells, and diabetes: the emperor has no clothes, Diabetes 69 (2020) 273–278, https://doi.org/10.2337/db19-0138.
[19] A.E. Butler, J. Janson, S. Bonner-Weir, R. Ritzel, R.A. Rizza, P.C. Butler, Beta-cell deficit and increased beta-cell apoptosis in humans with type 2 diabetes, Diabetes 52 (1) (2003) 102–110, https://doi.org/10.2337/diabetes.52.1.102.
[20] M. Masini, M. Bugliani, R. Lupi, et al., Autophagy in human type 2 diabetes pancreatic beta cells, Diabetologia 52 (6) (2009) 1083–1086, https://doi.org/10.1007/s00125-009-1347-2.
[21] M. Suleiman, L. Marselli, M. Cnop, et al., The role of beta cell recovery in type 2 diabetes remission, Int. J. Mol. Sci. 23 (13) (2022) 7435, https://doi.org/10.3390/ijms23137435.
[22] Z. Iqbal, G. Morahan, M. Arooj, A.N. Sobolev, S. Hameed, Synthesis of new arylsulfonylspiroimidazolidine-2',4'-diones and study of their effect on stimulation of insulin release from min6 cell line, inhibition of human aldose reductase, sorbitol accumulations in various tissues and oxidative stress, Eur. J. Med. Chem. 1682019) 154-175, https://doi.org/10.1016/j.ejmech.2019.02.036.
[23] E. Mukai, S. Fujimoto, N. Inagaki, Role of reactive oxygen species in glucose metabolism disorder in diabetic pancreatic β-cells, Biomolecules 12 (9) (2022) 1228, https://doi.org/10.3390/biom12091228.
[24] F.R. Palma, B.N. Gantner, M.J. Sakiyama, et al., Ros production by mitochondria: function or dysfunction? Oncogene 43 (5) (2024) 295–303, https://doi.org/10.1038/s41388-023-02907-z.
[25] I. Bratic, A. Trifunovic, Mitochondrial energy metabolism and ageing, Biochim. Biophys. Acta Bioenerg. 1797 (6–7) (2010) 961–967, https://doi.org/10.1016/j.bbabio.2010.01.004.
[26] Y. Lai, N. Yang, D. Shi, et al., Puerarin enhances tfeb-mediated autophagy and attenuates ros-induced pyroptosis after ischemic injury of random-pattern skin flaps, Eur. J. Pharmacol. 9742024) 176621, https://doi.org/10.1016/j.ejphar.2024.176621.
[27] D. Cai, Y. Zhao, F. Yu, Puerarin ameliorates acute lung injury by modulating nlrp3 inflammasome-induced pyroptosis, Cell Death Discov 8 (1) (2022) 368, https://doi.org/10.1038/s41420-022-01137-8.
[28] T.L. Rothstein, Signals and susceptibility to programmed death in b cells, Curr. Opin. Immunol. 8 (3) (1996) 362–371, https://doi.org/10.1016/S0952-7915(96)80126-9.
[29] H. Jin, Y.S. Ko, S.W. Park, K.C. Chang, H.J. Kim, 13-ethylberberine induces apoptosis through the mitochondria-related apoptotic pathway in radiotherapy-resistant breast cancer cells, Molecules 24 (13) (2019) 2448, https://doi.org/10.3390/molecules24132448.
[30] Y. Zhao, S. Zhang, P. Wang, S. Fu, D. Wu, A. Liu, Seleno-short-chain chitosan induces apoptosis in human non-small-cell lung cancer a549 cells through ros-mediated mitochondrial pathway, Cytotechnology 69 (6) (2017) 851–863, https://doi.org/10.1007/s10616-017-0098-z.
[31] C.M.K.S. Korsmeyer, Bcl-2 and bax function independently to regulate cell death, Nat. Genet. 161997) 358-363, https://doi.org/DOI:10.1038/ng0897-358.
[32] V. Andreu-Fernández, M. Sancho, A. Genovés, et al., Bax transmembrane domain interacts with prosurvival bcl-2 proteins in biological membranes, Proc. Natl. Acad. Sci. USA 114 (2) (2017) 310–315, https://doi.org/10.1073/pnas.1612322114.
[33] B.D. Sahu, S. Tatireddy, M. Koneru, et al., Naringin ameliorates gentamicin-induced nephrotoxicity and associated mitochondrial dysfunction, apoptosis and inflammation in rats: possible mechanism of nephroprotection, Toxicol. Appl. Pharmacol. 277 (1) (2014) 8–20, https://doi.org/10.1016/j.taap.2014.02.022.
[34] J. Jezek, K.T. Chang, A.M. Joshi, R. Strich, Mitochondrial translocation of cyclin c stimulates intrinsic apoptosis through bax recruitment, EMBO Rep. 20 (9) (2019) e47425, https://doi.org/10.15252/embr.201847425.
[35] F.J. Bock, S.W.G. Tait, Mitochondria as multifaceted regulators of cell death, Nat. Rev. Mol. Cell Biol. 21 (2) (2020) 85–100, https://doi.org/10.1038/s41580-019-0173-8.
[36] P.P. Praharaj, P.P. Naik, D.P. Panigrahi, et al., Intricate role of mitochondrial lipid in mitophagy and mitochondrial apoptosis: its implication in cancer therapeutics, Cell. Mol. Life Sci. 76 (9) (2019) 1641–1652, https://doi.org/10.1007/s00018-018-2990-x.
[37] V. Sorrentino, K.J. Menzies, J. Auwerx, Repairing mitochondrial dysfunction in disease, Annu. Rev. Pharmacol. Toxicol. 58 (1) (2018) 353–389, https://doi.org/10.1146/annurev-pharmtox-010716-104908.
[38] J.Y. Sun, Y.J. Hou, X.Y. Fu, et al., Selenium-containing protein from selenium-enriched spirulina platensis attenuates cisplatin-induced apoptosis in mc3t3-e1 mouse preosteoblast by inhibiting mitochondrial dysfunction and ros-mediated oxidative damage, Front. Physiol. 92018 (1907), https://doi.org/10.3389/fphys.2018.01907.
[39] L. Galluzzi, D.R. Green, Autophagy-independent functions of the autophagy machinery, Cell 177 (7) (2019) 1682–1699, https://doi.org/10.1016/j.cell.2019.05.026.
[40] K.S.C.M. Francesco P. Zummo, A.C. Arden, Glucagon-like peptide 1 protects pancreatic b-cells from death by increasing autophagic flux and restoring lysosomal function, Diabetes 66 (2017) 1272–1285. http://10.2337/db16-1009.
[41] Q. Bai, Z. Wang, Y. Piao, et al., Sesamin alleviates asthma airway inflammation by regulating mitophagy and mitochondrial apoptosis, J. Agric. Food Chem. 70 (16) (2022) 4921–4933, https://doi.org/10.1021/acs.jafc.1c07877.
[42] H.X. Peng, F. Chai, K.H. Chen, et al., Reactive oxygen species-mediated mitophagy and cell apoptosis are involved in the toxicity of aluminum chloride exposure in gc-2spd, Biol. Trace Elem. Res. (2023), https://doi.org/10.1007/s12011-023-03848-0.
[43] W. Ding, Y. Dong, X. Zhang, Globular adiponectin protects hepatocytes against intermittent hypoxia-induced injury via pink1/parkin-mediated mitophagy induction, Sleep Breath. 26 (3) (2022) 1389–1397, https://doi.org/10.1007/s11325-021-02508-8.
[44] Y. Hu, Y. Li, M. Li, et al., Calcium supplementation attenuates fluoride-induced bone injury via pink1/parkin-mediated mitophagy and mitochondrial apoptosis in mice, J. Hazard Mater. 465 (2024) 133411, https://doi.org/10.1016/j.jhazmat.2023.133411.
[45] M. Liu, X. Wu, Y. Cui, et al., Mitophagy and apoptosis mediated by ros participate in alcl3-induced mc3t3-e1 cell dysfunction, Food Chem. Toxicol. 155 (2021) 112388, https://doi.org/10.1016/j.fct.2021.112388.
[46] C. Zhu, Y. Zhao, D. Pei, et al., Pink1 mediated mitophagy attenuates early apoptosis of gingival epithelial cells induced by high glucose, BMC Oral Health 22 (1) (2022) 144, https://doi.org/10.1186/s12903-022-02167-5.
[47] T. Lamark, V. Kirkin, I. Dikic, T. Johansen, Nbr1 and p62 as cargo receptors for selective autophagy of ubiquitinated targets, Cell Cycle 8 (13) (2009) 1986–1990, https://doi.org/10.4161/cc.8.13.8892.
[48] S. Shao, C.B. Xu, C.J. Chen, et al., Divanillyl sulfone suppresses nlrp3 inflammasome activation via inducing mitophagy to ameliorate chronic neuropathic pain in mice, J. Neuroinflammation 18 (1) (2021) 142, https://doi.org/10.1186/s12974-021-02178-z.
[49] Y. Yang, D. Xing, F. Zhou, Q. Chen, Mitochondrial autophagy protects against heat shock-induced apoptosis through reducing cytosolic cytochrome c release and downstream caspase-3 activation, Biochem. Biophys. Res. Commun. 395 (2) (2010) 190–195, https://doi.org/10.1016/j.bbrc.2010.03.155.